Journal of Hazardous Materials, 11 (1985) 325—340
Elsevier Science Publishers B.V., Amsterdam — Printed in The Netherlands

UNSTEADY GRAVITY CURRENT FLOWS OVER OBSTACLES: SOME OBSERVATIONS AND ANALYSIS RELATED TO THE PHASE II TRIALS

JAMES W. ROTTMAN, JOHN E. SIMPSON, J.C.R. HUNT

Department of Applied Mathematics and Theoretical Physics, University of Cambridge, Silver Street, Cambridge CB3 9EW (Great Britain)

and R.E. BRITTER

Department of Engineering, University of Cambridge, Trumpington Street, Cambridge CB2 1PZ (Great Britain)

(Received July 20, 1984; accepted August 28, 1984)

Summary

The Phase II trials at Thorney Island were designed to provide a few full-scale results of the interaction of heavy gas clouds with surface-mounted obstacles. In this paper, we interpret some preliminary observations from the Phase II trials by reviewing and developing the theory of two-layer fluid flows over obstacles and comparing these results with visual observations of the field trials. The results are preliminary, and largely qualitative, because the concentration and other quantitative measurements are not yet available.

1. Introduction

Accidents involving the release of dangerous heavy gases may occur amongst groups of obstacles, such as buildings, storage tanks or trees. Also obstacles such as solid or porous fences may be used to help contain accidental releases of heavy gases or enhance their dispersion. The Phase II trials at Thorney Island were designed to provide a few benchmark experiments of heavy gas flows near surface-mounted obstacles with which wind-tunnel simulations can be validated. Our purpose in this paper is to review and develop the theory of two-layer fluid flows over obstacles and to compare the results of this theory with some preliminary observations from the Phase II trials.

Three different types of obstacle were used in the Phase II trials:

(1) a 5 m high solid fence arranged in a semicircle of radius 50 m around the downwind side of the release centre,
(2) a 10 m high porous fence similarly arranged, and
(3) a cube with sides 9 m in length placed 50 m downwind of the release centre at various angles to the mean wind direction.

In one of the experiments the cube was placed upwind of the release centre.

0304-3894/85/$03.30

In all, only ten trials were performed, four with the solid fence, two with the porous fence, and four with the cube. More complete details of the Phase II trials are given in [1].

For each type of obstacle, we develop some simple theoretical and computational models to help interpret the observations, and we report the results of some simple laboratory experiments in a water channel. Our observations are based on the video and still camera records of the trials, the sensor measurements not yet being available. As there were only ten full-scale trials, it is not possible to draw any general conclusions, but we hope that our interpretation will be helpful in gaining a broad insight into these complicated flows.

2. Gravity current flow over a solid fence

Our concern is mainly with the transient interaction of the released gravity current with the fence. Near the centre of the semi-circular fence the flow might be approximated as two-dimensional during the interaction. In Section 2.1 the two-dimensional steady-flow hydraulic analysis used to design the field experiments is outlined [2]. In Section 2.2 we examine how much unsteady hydraulic analysis can tell us about the transient aspects of the flow, and finally in Section 2.3 we describe some qualitative laboratory experiments in a parallel-sided water channel.

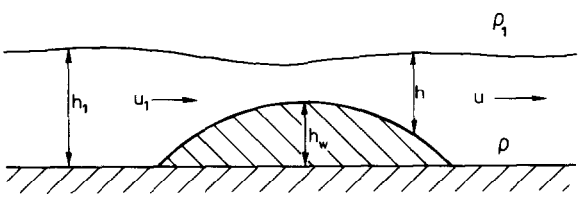

Fig. 1. Schematic diagram of shallow two-layer flow over an obstacle.

2.1 Steady hydraulic analysis

Consider the flow over an obstacle of height h_w of a two-layer fluid, as illustrated in Fig. 1. The lower layer has density ρ and depth h whereas the upper layer has infinite depth and density ρ_1. The motion of the upper fluid can be ignored in the shallow-water approximation and the motion in the lower layer is governed by the equations

$$\frac{\partial h}{\partial t} + \frac{\partial}{\partial x}(uh) = 0, \tag{2.1}$$

$$\frac{\partial u}{\partial t} + u\frac{\partial u}{\partial x} + g'\frac{\partial}{\partial x}(h_w + h) = 0, \tag{2.2}$$

where

$$g' = g\left(\frac{\rho - \rho_1}{\rho_1}\right) \tag{2.3}$$

is the reduced acceleration due to gravity. The symbol u in these equations represents the horizontal fluid speed vertically averaged over the lower layer. These equations are derived by Houghton and Kasahara [3] among many others.

Steady solutions to these equations are sought by setting the partial derivatives with respect to time equal to zero. The equations then reduce to

$$uh = u_1 h_1 \tag{2.4}$$

$$\frac{u^2}{2g'} = h_w + h = \frac{u_1^2}{2g'} + h_1 \tag{2.5}$$

where u_1 and h_1 are the upstream values of u and h. In [3] it is shown that solutions to these last two equations only exist in the regions exterior to the curve BAF in Fig. 2, i.e. the two regions labelled sub-critical and super-critical flow. Inside this curve, the solutions are unsteady. But observations show that in a neighbourhood about the obstacle (a neighbourhood whose size increases with time), the flow is steady, but it requires energy to be dissipated by hydraulic jumps in order to match this inner steady solution to the upstream and downstream conditions. The different possible flow configurations and the regions in the parameter space for which they exist are indicated in Fig. 2 (from [4]).

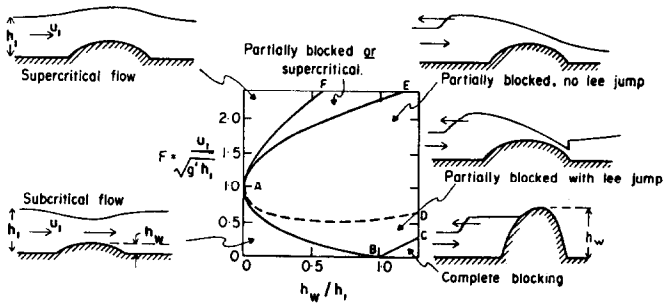

Fig. 2. The flow regime for shallow-water flow over an obstacle. F is the Froude number of the upstream flow and h_w is the maximum height of the obstacle (from [4]).

The particular flow regime we are interested in is defined by the lower right-hand corner of Fig. 2, where the flow is either partially or completely blocked. The equation for the curve delineating partially from completely-blocked flow is given in [3] as

$$\frac{u_1^2}{g'h_1} = \frac{1}{2}(H_w - 1)^2\left(\frac{H_w + 1}{H_w}\right), \tag{2.6}$$

where $H_w = h_w/h_1$. Below this line the flow is completely blocked and above this line only partially blocked. By the term blocked, we mean that no fluid flows over the barrier and a hydraulic jump propagates upstream. Partially blocked means that a hydraulic jump propagates upstream and fluid flows over the barrier. These two cases are illustrated in Fig. 2.

The flow of interest in the present context is sketched in Fig. 3. The figure shows a constant upstream depth h_1 and speed u_1, a hydraulic jump propagating upstream with speed U and a downstream depth h_2 and speed u_2, and finally the critical flow over a wall of height h_w. The conditions that must be satisfied at the jump are [5]:

$$(u_1 - U)h_1 = (u_2 - U)h_2\,, \tag{2.7}$$

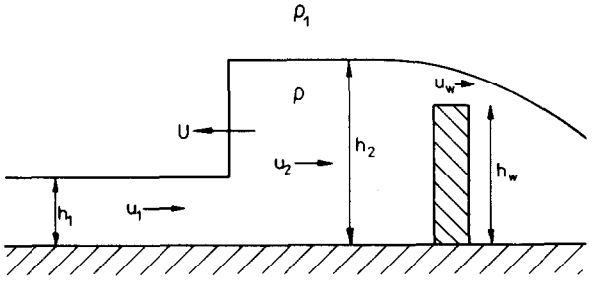

Fig. 3. Schematic illustration of shallow-water flow over a wall, showing the hydraulic jump propagating upstream away from the wall.

$$(u_1 - U)^2 = \frac{1}{2}\,(g'h_1)\frac{h_2}{h_1}\left(1 - \frac{h_2}{h_1}\right). \tag{2.8}$$

These conditions ensure that mass and momentum are conserved through the jump, and the requirement $h_2 > h_1$ ensures that energy is dissipated. We assume that the flow over the wall is critical; that is,

$$u_w = \sqrt{g'\Delta h}\,, \tag{2.9}$$

where u_w is the depth-averaged speed of the fluid flowing over the wall and $\Delta h = h_2 - h_w$.

Using mass conservation we can express (2.9) in terms of u_2 as

$$u_2^2 = \begin{cases} (g'h_2)(1 - h_w/h_2)^3 & \text{if } h_w/h_2 < 1 \\ 0 & \text{if } h_w/h_2 \geqslant 1 \end{cases}. \tag{2.10}$$

The relations (2.7), (2.8) and (2.10) can be combined to yield two equations for $H_b = h_w/h_1$ and U in terms of the given quantities $u_1/\sqrt{g'h_1}$ and $H_w = h_w/h_1$:

$$u_1 - (1 - H_b)U = (g'h_1)^{1/2}\,[H_b(1 - H_w/H_b)]^{3/2} \tag{2.11}$$

$$(u_1 - U)^2 = \frac{1}{2}\,(g'h_1)H_b(1 + H_b)\,, \tag{2.12}$$

if $h_w/h_2 < 1$, and

$$u_1 = (1 - H_b)U \tag{2.13}$$

$$U^3 = u_1 U^2 - (g'h_1)^{1/2}U + \frac{1}{2}(g'h_1)^{1/2}u_1 = 0\,, \tag{2.14}$$

if $h_w/h_2 \geqslant 1$.

Solutions of these equations in the relevant parameter range are plotted in Fig. 4. The values of $u_1/(g'h_1)^{1/2}$ shown in the plot are those appropriate for most gravity currents. A general conclusion that may be drawn from this plot is that $1.5 < h_2/h_1 < 2.5$ for most cases of interest, and a good rule of thumb is that $h_2/h_1 \approx 2$.

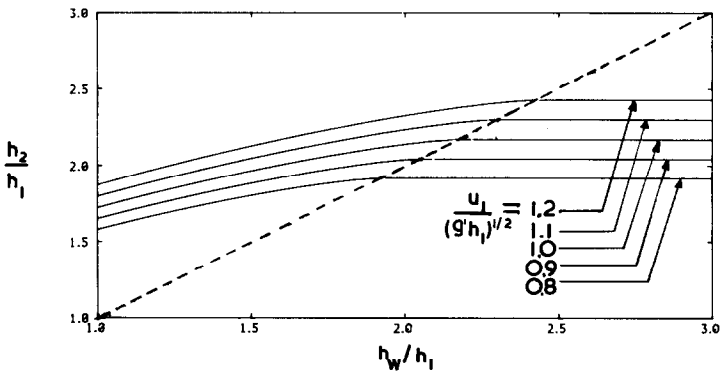

Fig. 4. Solutions of the steady shallow-water equation for the depth of the fluid behind the hydraulic jump as a function of the wall height h_w, as illustrated in Fig. 3. The flow is blocked in the region to the right of the dashed line and partially blocked in the region of the left.

The analysis described in the present section is essentially for the fluid motion *after* the gravity current has interacted with the wall and a steady flow in a neighbourhood about the wall has been established. In the next section, we examine the unsteady interaction of the gravity current front with the wall. The points of interest are how long after the current first meets the wall is the steady state established and how high does the current rise up the wall. We specifically consider what unsteady hydraulics can tell us about these questions.

2.2 Unsteady hydraulic analysis

We now show how the unsteady interaction of the gravity current with the barrier can be computed using the shallow-water approximation. This is particularly simple if we make the additional assumption that h_2 remains level (constant) during the interaction. From our experiments, to be described later, this seems to be fairly accurate for the bulk of the fluid. A similar assumption was made by Greenspan and Young [6] in their analysis of liquid-in-air flow over barriers.

A sketch of the flow under consideration is shown in Fig. 5. If we take the height $h_1(x,t)$ as given, then the continuity equation in integral form, after the current meets the wall, is

$$\int_{x_s(t)}^{u_f t} h_1 \, dx = \int_{x_s(t)}^{x_w} h_2 \, dx \,, \tag{2.15}$$

and if we assume that h_2 is a function of time only, we obtain an equation for $h_2(t)$:

$$h_2(t) = [x_w - x_s(t)]^{-1} \int_{x_s(t)}^{u_f t} h_1(x,t) dx \,, \tag{2.16}$$

where $x_s(t)$ is the position of the hydraulic jump and x_w is the position of the barrier. Then, since $dx_s/dt = U$, we obtain an ordinary differential equation for $x_s(t)$ from (2.8):

$$\frac{dx_s}{dt} = u_1 - \frac{1}{\sqrt{2}} (g' h_1)^{1/2} [H_b(1 + H_b)^3]^{1/2} \,, \tag{2.17}$$

where $H_b(t) = h_2(t)/h_1[x = x_s(t),t]$.

This equation can be integrated for specified $h_1(x,t)$ and $u_1(x,t)$ and it gives the time until the steady state, as derived in the previous section, is

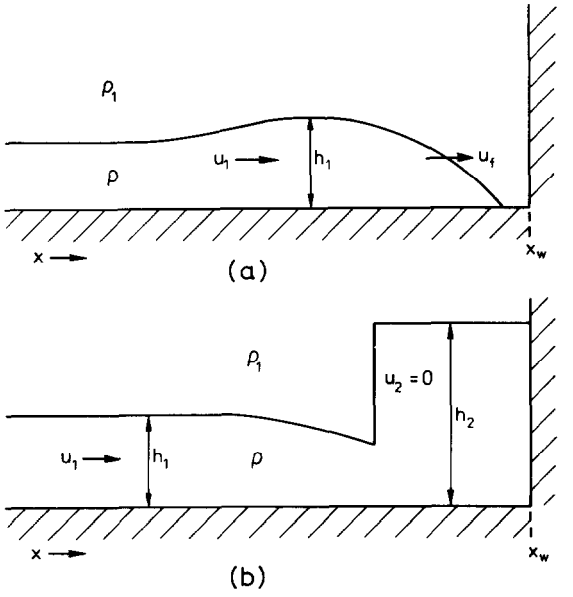

Fig. 5. Schematic illustration of the transient interaction of a gravity current with a solid vertical wall: (a) before the interaction; (b) after the interaction, with a hydraulic jump propagating away from the wall.

achieved after the current first meets the wall. This gives an indication of the time of the interaction, but it requires some knowledge of the structure of the gravity current front.

However hydraulic theory is not valid at the current front (where vertical accelerations are large), nor can it predict the rapid vertical motion that is certain to occur when the current impacts the wall. Indeed, the experiments to be described later show an initial jet of fluid that shoots up the wall at the initial impact. So, such an analysis would be able to predict the motion of the bulk of the fluid, but not of the small amount of fluid with large vertical accelerations — the "splash" as seen in the field tests (to be described later).

Dimensional analysis shows that the duration of the interaction is given by

$$t_* = \alpha(h_1/g')^{1/2}, \tag{2.18}$$

where α is some O(1) constant. In the next section we describe some laboratory experiments in a water channel that enables us to estimate the value of α.

To compute the initial "splash" up the wall would require the numerical solution of the fully nonlinear Euler equations. That would be a very difficult task for such a complicated flow as a gravity current front. We chose the simpler approach of performing some descriptive laboratory experiments to study the initial "splash", as described in the next section.

2.3 Laboratory experiments

The experiments were performed in a parallel-sided channel, 20.5 cm wide, 50 cm deep and 348 cm long. The channel was filled with tap water and then salt water was pumped into the bottom of the tank to a depth of 10 cm in a lock with a Perspex gate 70 cm from the end of the tank. Barriers of different heights were placed 70 cm from the Perspex gate. The experiments were initiated by removing the Perspex gate, allowing the heavy fluid to flow along the bottom of the tank. This technique is identical to that used in [7] and as described in that paper it generates a gravity current that propagates steadily for 4 lock lengths. Thus, one obtained a steady gravity current interacting with the barrier. The experiments were recorded on video tape, from which all measurements were taken.

Figure 6 is a series of photographs showing the interaction of the current with an "infinitely high" barrier. Note the high "splash" of heavy fluid that runs up the wall to about twice the original height of the released fluid (indicated by a dark horizontal line in the photographs). This fluid is very dilute, and it is clear from the photographs that the bulk of the heavy fluid only rises to the 10 cm mark, or about twice the height of the gravity current. The later photographs show a 10 cm high hydraulic jump moving away from the barrier. It seems from these experiments that the shallow-water analysis is adequate to predict the motion of the bulk of the heavy fluid,

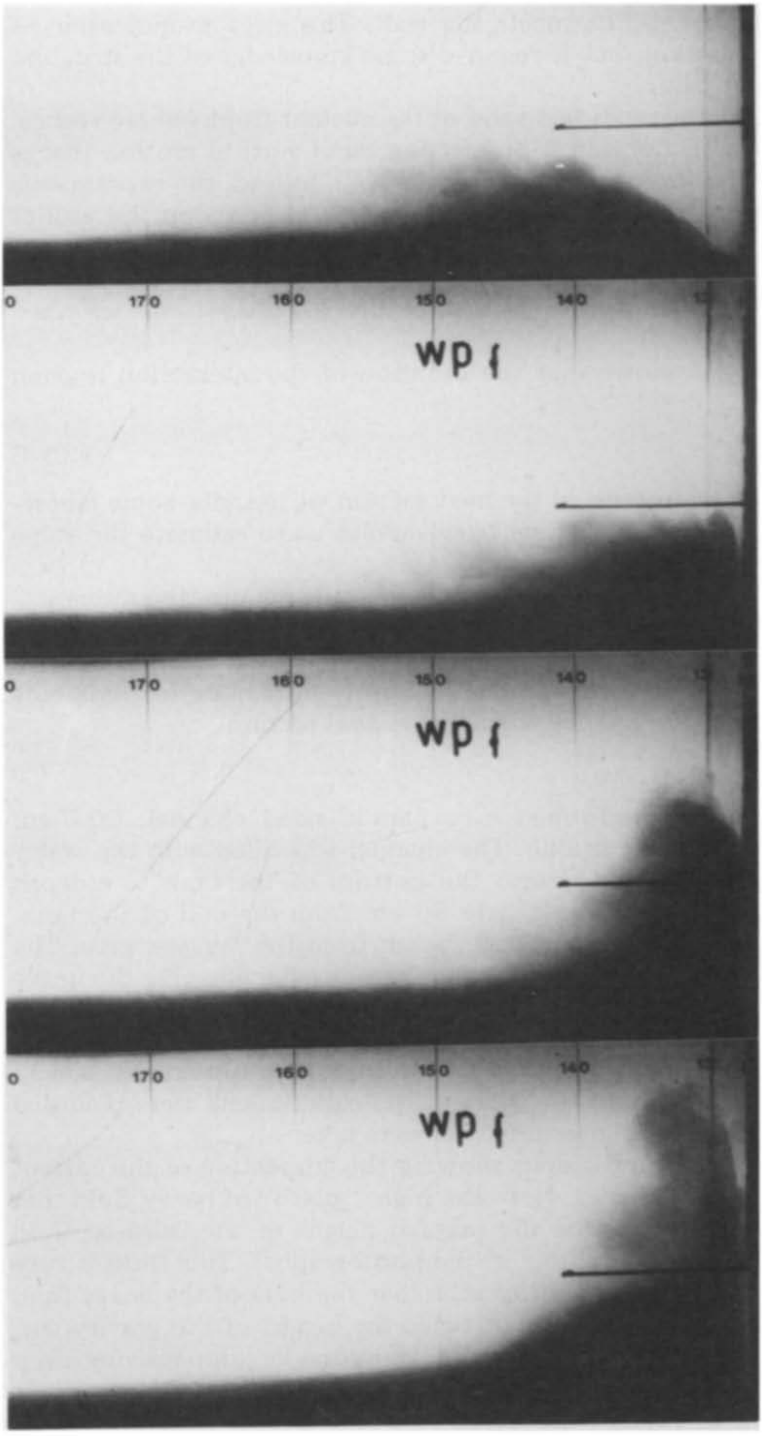
0
17.0
16.0
15.0
14.0
wp 1
0
17.0
16.0
15.0
14.0
wp 1
0
17.0
16.0
15.0
14.0
wp 1

but incapable of predicting the "splash" of very dilute fluid. Measurements of the time after initial encounter with the wall until the formation of a steady hydraulic jump gives $\alpha \approx 5$.

Figure 7 is a series of photographs showing the interaction of a gravity current with a 5 cm high fence, which is about the same height as the gravity current. Again an amount of fairly dilute fluid shoots up the wall in the form of a jet, but the bulk of the fluid surmounts the fence, reforming into a gravity current on the other side of the fence while a hydraulic jump propagates away from the fence in the opposite direction. Again, the eventual steady state with the heavy fluid flowing over the fence is qualitatively consistent with the steady hydraulic analysis. Again, it is found that $\alpha \approx 5$.

3. Gravity current flow through a porous fence

As described in more detail in [1], the porous fence in the field trials consisted of scaffolding across which was stretched army camouflage netting. The detailed characteristics of this netting have not been determined, but it is sufficient for our purposes to treat it as a region of increased flow resistance. Here we consider first the steady hydraulic effects of a region of increased flow resistance on a steady gravity current, then we offer a few remarks about the transient effects, and finally we describe some simple water-channel experiments. As with the solid fence, we only consider two-dimensional flows.

3.1 Steady hydraulic analysis with a region of increased flow resistance

For steady undirectional flow where the height is a slowly varying function of the horizontal coordinate x, standard hydraulic analysis (see, for example [8]) gives the following relation between the slope of the interface

$$\frac{dh}{dx} = -\frac{C_D F^2}{1 - F^2} \tag{3.1}$$

where

$$F^2 = (uh)^2/g'h^3 \tag{3.2}$$

is the local Froude number of the flow and $C_D u^2$ is the drag per unit flow area.

In steady gravity currents moving along a rigid horizontal bottom the flow resistance is mostly due to the friction at the bottom and at the interface between the two fluids. The observed form of such gravity currents is sketched in Fig. 8. Near the front of the current the depth-averaged Froude

Fig. 6. Sequential photographs of a laboratory experiment in a parallel-sided water channel showing the interaction of a gravity current with a solid wall of "infinite" height. The horizontal line indicates a height approximately twice that of the approaching gravity current.

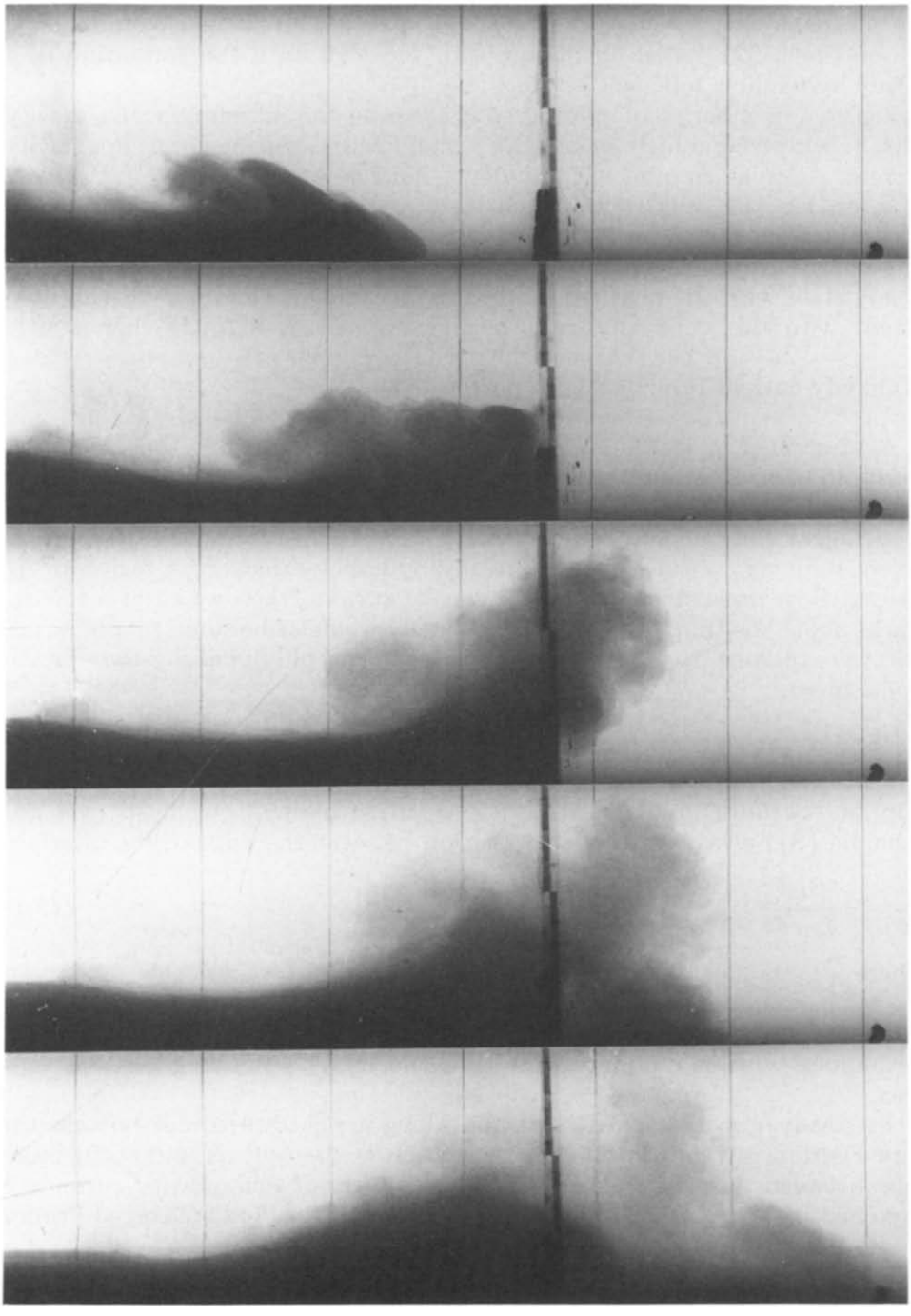

Fig. 7. Sequential photographs of a laboratory experiment in a parallel-sided water channel showing the interaction of a gravity current with a 5 cm high solid wall (about the same height as the approaching gravity current).

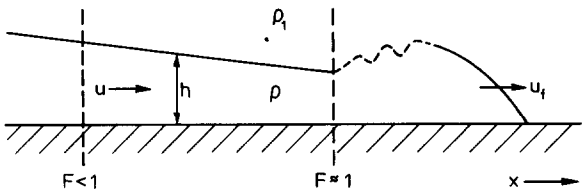

Fig. 8. Schematic illustration of a gravity current identifying the values of the Froude number in different regimes of the flow.

number is about unity, and there the depth of the current changes very abruptly. Farther behind the current front, the depth-averaged Froude number is less than unity, and consistent with (3.1) the interface slope is observed to be negative.

Thus if a region of increased flow resistance lies in the path of a gravity current, it will be distorted as sketched in Fig. 9. Since the depth-averaged Froude number is less than unity, we expect the slope of the interface to become more negative through the region of increased resistance. The total flow rate is still controlled by the gravity current front which determines the downstream boundary condition.

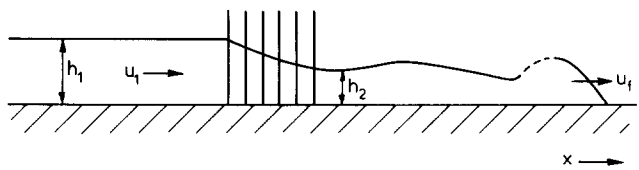

Fig. 9. Schematic illustration of a gravity current flowing through a porous obstacle (indicated by a series of vertical lines).

The total problem, after the transient effects have disappeared, could be solved by a method similar to that used in Section 2.1 for the solid fence. In an expanding region about the porous barrier, the flow becomes steady and this steady flow region can be patched onto the upstream and downstream boundary conditions with hydraulic jumps or long waves. The downstream boundary condition is determined by the gravity front, whereas the upstream condition is the same as in the solid fence problem.

3.2 Transient effects with a region of increased flow resistance

Here we only offer a few thoughts about the transient interaction of a gravity current with a region of increased flow resistance in anticipation of the experiments that are described in the next section. By analogy with the solid fence, we might expect the gravity current front initially to increase in height and for a hydraulic jump to form and propagate back along the gravity current as the flow adjusts to a steady state. Of course since the fence

is porous, we would not expect the current front height to increase as much as the case of a solid fence, nor would we expect as much diluted fluid to shoot well above the wall in the form of a jet. The strength of the interaction will be a function of the porosity of the wall.

3.3 Experiments on gravity currents flowing through a porous barrier

The experiments were performed in the same apparatus as described in Section 2.3, using the same technique for generating a steady gravity current. In this case, the fence was replaced by a 5 cm long by 20 cm wide barrier consisting of 40 equally-spaced 10 mm diameter wooden dowels, each 10 cm in height. We made no attempt to estimate the drag coefficient associated with the barrier, because the experiments are only intended to be of a qualitative nature. Its porosity (the volume of the dowels divided by the total volume off the barrier) is about 0.3.

Figure 10 is a series of photographs showing the interaction of a steady gravity current with our porous barrier. As we anticipated in the previous section, the gravity current increases in height as it first encounters the barrier. It can be seen that its height nearly doubles. The speed of the front is also retarded. Soon, however, the heavy fluid seeps through at the bottom of the barrier and begins to reform a gravity current front, while at the same time a weak hydraulic jump propagates upstream from the barrier. The "splash" associated with the initial interaction is much weaker, as expected, than for the case with the solid fence. Eventually, a steady state is achieved with a rapid drop in the interface level through the barrier with a gravity current front propagating downstream away from the barrier.

4. Gravity current interaction with a cube

What follows are a few brief remarks about what might be expected when a gravity current encounters a solid cube. The main feature of this sutuation that is different from the previous two cases is that now the heavy fluid can go around the obstacle as well as over it. In this sense, the steady aspects of the flow are similar in nature to stratified flows over isolated hills.

The flow of a continuously stratified fluid near an isolated hill has been studied extensively, e.g. [9—11]. Study of the more relevant (in the present context) flow with two-layer stratification is less frequent. However in [9] it is argued that when the dense cloud depth h is less than the hill (or cube) height H the interface will rise by $\frac{1}{2}(U^2/g')$ as it stagnates on the cube, where U is the current speed. When the Froude number $[U^2/g'H]^{1/2} \ll 1$, the dense cloud will travel entirely around the cube. The cloud will separate on the downwind side of the cube, creating a mainly horizontal recirculating flow. During the initial transient interactions we expect that there will be a "splash" of fluid up the face of the cube on initial impact, but the splash should not go as high as in the case with the solid fence if the dimensions of the cube are not much greater than the height of the current.

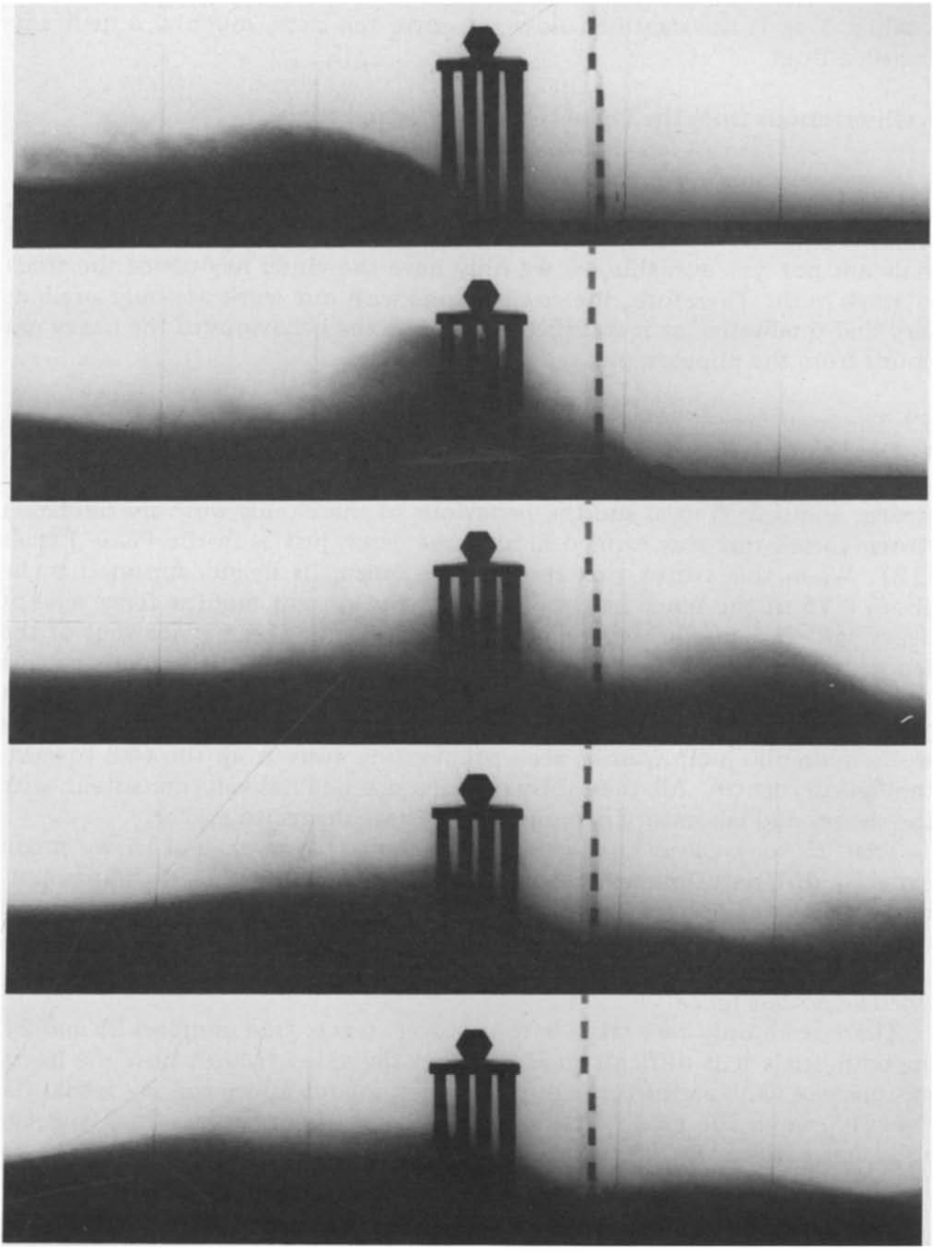

Fig. 10. Sequential photographs of a laboratory experiment in a parallel-sided water channel showing the interaction of a gravity current with a porous obstacle. The porous obstacle consists of 40 wooden rods, 10 mm in diameter and 10 cm high, evenly spaced over a region 20 cm wide and 5 cm long.

When $F \gg 1$, the stratified flow goes over the cube, much as a neutrally stratified fluid.

5. Observations from the Phase II Thorney Island trials

We report some qualitative observations from the Phase II trials and compare them with the theory and laboratory experiments described in the previous sections. As stated earlier, the quantitative data from the Phase II trials are not yet available, so we only have the visual records of the trials to work with. Therefore, the comparisons with our work are only preliminary and qualitative as it is difficult to define the behaviour of the heavy gas clouds from the photographs and video records.

5.1 The solid fence

The trial numbers for the field experiments with a solid fence are 20, 21, 22 and 25. In the first three of these trials the ambient wind was fairly strong, about 3—5 m/s, and the behaviour of the clouds was very similar. A strong vortex ring was formed in all three cases, just as in the Phase I trials [12]. When this vortex ring reached the fence, its height appeared to be about 0.75 of the fence height. Just after the current met the fence a jet of heavy gas shot up the fence and reached a height about twice that of the fence; some very faint wisps of smoke reached nearly three fence heights into the air. But it appears that the bulk of the fluid only reached about twice the height of the vortex ring. In all three trials a weak wave, or perhaps weak hydraulic jump, can be seen propagating away from the wall towards the release centre. All these observations are qualitatively consistent with the theory and laboratory experiments we have described earlier.

Trial 25 took place in a weak wind (about 1.5 m/s), and so we might expect a different flow behaviour than in the other three cases. Unfortunately, the trial was performed late in the evening and the video records are too dark to discern any of the details of the motion.

5.2 The porous fence

There were only two trials with a porous fence: trial numbers 23 and 24. In both trials it is difficult to judge from the video records how the heavy gas behaves as it passes through the barrier. About all we can say is that the "splash" when the cloud first meets the barrier is much less than with the solid fence, even though the crosswind was much stronger (5—7 m/s) in the porous fence trials. Unfortunately we cannot be more quantitative.

5.3 The cube

There were four trials with the cube: trial numbers 26, 27, 28 and 29. In Trial 29 the cube was placed upwind of the containment vessel. The visual records of this trial are not very useful since the gas was released after sunset and it was quite dark. Trials 26 and 27 were performed in light winds (1—2

m/s) and the cloud remained horizontal as it went around the cube in each of those trials. There was very little observable splash in these cases. In Trial 28 the wind was very strong (9 m/s) and the cloud appears as if it diffuses passively. The cloud acts as a passive flow tracer as it flows past the cube with no obvious dense gas effects. These observations are consistent with our discussion in Section 4. If we approximate the specific gravity of the current when it reaches the cube as about 1.1 and the current speed as roughly equal to the wind speed, then the parameter $(U^2/g'H)^{1/2}$ is about 1/3 for Trials 26 and 27 and about 3 for Trial 28.

6. Concluding remarks

We have attempted to gain some insight into heavy gas flows over obstacles by studying theoretically and experimentally a few idealised problems that are related to the Phase II trials. The comparison of our results with the actual trials is limited because the quantitative measurements from the trials are not yet available. From the available visual records, the results we have obtained seem to be consistent with the field trials and give physical reasons for why the flow behaves as it does.

For the case with a solid fence we have shown that two-dimensional hydraulic theory predicts that the bulk of the heavy fluid should rise to approximately twice the height of the current when it meets the wall. Our laboratory experiments confirm this result. Hydraulic theory cannot predict the jet of fluid that rises much higher, but our experiments show that this fluid is quite dilute.

For the case with a porous fence, hydraulic analysis suggests that the interface declines as it passes through the fence. Our laboratory experiments show that this is true and that the current reforms into a gravity current front after it passes through the fence. We outlined methods that could be used to determine the entire problem of steady gravity current flow through a region of increased flow resistance.

Finally, we gave estimates based on the theory of steady stratified flow around hills of under what conditions under which a heavy gas cloud flows around an isolated obstacle or goes over it.

Acknowledgements

The authors acknowledge financial support from the U.K. Health and Safety Executive under contract 1918/01.01 (J.W.R.) and from the U.K. Atomic Energy Authority, Safety and Reliability Directorate (R.E.B.).

References

1 M.E. Davies and S. Singh, The Phase II trials: a data set on the effect of obstructions, J. Hazardous Materials, 11 (1985) 301—323.
2 J. McQuaid, personal communication, 1984.

3 D.D. Houghton and A. Kasahara, Nonlinear shallow fluid flow over an isolated ridge, Comm. Pure Appl. Math., 21 (1968) 1—23.
4 P.G. Baines and P.A. Davies, Laboratory studies of topographic effects in rotating and/or stratified flows, in: Orographic Effects in Planetary Flows, GARP, publication Series No. 23, World Meteorological Organization, 1980, pp. 233—299.
5 J.J. Stoker, Water Waves, Interscience, New York, 1957.
6 H.P. Greenspan and R.E. Young, Flow over a containment dyke, J. Fluid Mech., 87 (1978) 179—192.
7 J.W. Rottman and J.E. Simpson, Gravity currents produced by instantaneous releases of a heavy fluid in a rectangular channel, J. Fluid Mech., 135 (1983) 95—110.
8 J.S. Turner, Buoyancy Effects in Fluids, Cambridge University Press, Cambridge, 1973.
9 W.H. Snyder, R.E. Britter and J.C.R. Hunt, A fluid modelling study of the flow structure and plume impingement on a three-dimensional hill in a stably stratified flow, in: J.E. Cermak (Ed.), Proc. 5th Int. Conf. on Wind Engineering, Ft. Collins, Colo., 1979, Pergamon, Oxford, 1980.
10 J.C.R. Hunt and W.H. Snyder, Experiments on stably or neutrally stratified flow over a model three-dimensional hill, J. Fluid Mech., 96 (1980) 671—704.
11 P.W.M. Brighton, Strongly stratified flow past three-dimensional obstacles. Q.J. Roy. Met. Soc., 104 (1982) 289—307.
12 J.W. Rottman, J.C.R. Hunt and A. Mercer, The initial and gravity-spreading phases of heavy gas dispersion: comparison of models with Phase I data, J. Hazardous Materials, 11 (1985) 261—279.